

## Band gap engineering strategy via polarization rotation in perovskite ferroelectrics

Fenggong Wang, Ilya Grinberg, and Andrew M. Rappe

Citation: *Applied Physics Letters* **104**, 152903 (2014); doi: 10.1063/1.4871707

View online: <http://dx.doi.org/10.1063/1.4871707>

View Table of Contents: <http://scitation.aip.org/content/aip/journal/apl/104/15?ver=pdfcov>

Published by the [AIP Publishing](#)

---

### Articles you may be interested in

[Piezoelectric anisotropy of orthorhombic ferroelectric single crystals](#)

*J. Appl. Phys.* **113**, 224105 (2013); 10.1063/1.4809980

[Engineering polarization rotation in ferroelectric bismuth titanate](#)

*Appl. Phys. Lett.* **102**, 182901 (2013); 10.1063/1.4804367

[Strain sensitivity of polarization in perovskite ferroelectrics](#)

*Appl. Phys. Lett.* **93**, 122903 (2008); 10.1063/1.2988263

[Domain engineering of the transverse piezoelectric coefficient in perovskite ferroelectrics](#)

*J. Appl. Phys.* **98**, 014102 (2005); 10.1063/1.1929091

[Diffuse dielectric anomaly in perovskite-type ferroelectric oxides in the temperature range of 400–700°C](#)

*J. Appl. Phys.* **94**, 1904 (2003); 10.1063/1.1589595

---



**physicstoday**

Comment on any  
*Physics Today* article.

Physics Today / Volume 63 / Issue 10 / October 2012  
Previous Article | Next Article  
**Measured energy in Japan**  
David von Seggern  
(vonneg@seismo.unr.edu) University of Nevada  
July 2012, page 10  
DIGITAL OBJECT IDENTIFIER  
<http://dx.doi.org/10.1063/PT.3.1619>  
The article by Thome Lay and Hiroo Kanamori is an estimate of the energy released by the 2011 Tohoku earthquake. While that of a 100-megaton atmospheric explosion is approximately five times as much energy as that of a 100-megaton nuclear detonation event—a 20-megaton atmospheric explosion had 200 times more energy by a factor of about 3, or 10 times more energy than that of a 100-megaton nuclear device. I believe the authors used the relation for seismic energy release rather than total strain energy release. The seismic energy underestimates the total strain energy release by a variable that depends on friction on the fault plane. Accounting for total strain energy release would increase the earthquake energy number by orders of magnitude.  
Despite the catastrophic damage potential of nuclear bombs, the forces of nature occasionally unleash much larger energy releases. Although the nuclear bombs are under our control, earthquakes, volcanic eruptions, and extreme weather events are not. However, by judicious preparation and avoidance measures, humans can significantly diminish the damage of natural events.  
This article does not have any references.

**Comment on this article**  
By the act of hitting a ball with a bat, one calculates the force energy to deliver the ball to its new location, but one must also take into account that the ball extended its energy release to that which became struck by the ball as its momentum ceased and passed energy to the struck item. Therefore the parameters of the damage extend into the future when the received energy to that pushed upon, later becomes released in a new event. Perhaps calculations of one added that in while another's calculations did not. E.M.C.  
Written by Edgar Mocarville, 14 July 2012 19:59

## Band gap engineering strategy via polarization rotation in perovskite ferroelectrics

Fenggong Wang,<sup>a)</sup> Ilya Grinberg, and Andrew M. Rappe<sup>b)</sup>

The Makineni Theoretical Laboratories, Department of Chemistry, University of Pennsylvania, Philadelphia, Pennsylvania 19104-6323, USA

(Received 13 March 2014; accepted 6 April 2014; published online 16 April 2014)

We propose a strategy to engineer the band gaps of perovskite oxide ferroelectrics, supported by first principles calculations. We find that the band gaps of perovskites can be substantially reduced by as much as 1.2 eV through local rhombohedral-to-tetragonal structural transition. Furthermore, the strong polarization of the rhombohedral perovskite is largely preserved by its tetragonal counterpart. The *B*-cation off-center displacements and the resulting enhancement of the antibonding character in the conduction band give rise to the wider band gaps of the rhombohedral perovskites. The correlation between the structure, polarization orientation, and electronic structure lays a good foundation for understanding the physics of more complex perovskite solid solutions and provides a route for the design of photovoltaic perovskite ferroelectrics. © 2014 AIP Publishing LLC. [<http://dx.doi.org/10.1063/1.4871707>]

Solar energy is widely viewed as a long term substitution of the traditional fossil fuels because it is clean, abundant, and renewable.<sup>1</sup> In the past few decades, considerable efforts have been made to design and optimize materials for photocatalytic or photovoltaic use with the aim of efficiently converting light to electrical energy. This requires sufficient absorption of the solar radiation, efficient separation of the photo-excited charge carriers, and a low charge recombination rate. Ferroelectrics (FEs) provide a route to separate charge by the bulk photovoltaic effect, where charge carriers are separated spontaneously by a single phase material.<sup>2-4</sup> However, most of the current FE oxides have wide band gaps ( $E_g > 2.7$  eV for BiFeO<sub>3</sub>,  $E_g > 3.5$  eV for PZT) that are beyond the visible-light range and thus allow the use of only 8%–20% of the solar spectrum. Very recently, visible-light absorbing FEs have been reported,<sup>5,6</sup> and materials design of FEs with low band gaps in the visible-light range is still of crucial importance for their use in solar energy applications.

Perovskites (ABO<sub>3</sub>) are the most well-studied class of ferroelectrics for solar energy and other applications. They are not only capable of hosting above 90% of the natural metallic elements, but are also highly tunable through substitution and/or mixed oxidation states. As a result, they can exhibit a variety of interesting bulk and interfacial properties, ranging from the ferroelectric, magnetic, superconducting, and catalytic properties to the two dimensional electron gas.<sup>7,8</sup> Understanding the underlying physical properties of perovskites especially the correlation between the composition, structure, and electronic properties is highly desired for the design of efficient solar energy absorbers and bulk photovoltaics. There have been several studies demonstrating that O<sub>6</sub> tilting distortions from the ideal high-symmetry cubic ABO<sub>3</sub> structure have a strong impact on the band gaps of perovskites.<sup>9,10</sup> On the other hand, the impact of ferroelectric cation off-center displacements on  $E_g$  has been largely ignored. Here, we find that the BO<sub>6</sub> octahedral distortions induced by

the *B*-cation off-center displacements have a strong effect on the band gap and propose a strategy to reduce the band gaps of perovskites while maintaining their polarizations by rhombohedral (*R*)-to-tetragonal (*T*) structural transitions.

We performed first principles plane-wave density functional theory (DFT) calculations within the generalized gradient approximation (GGA) Perdew-Burke-Ernzerhof (PBE) approach,<sup>11,12</sup> as implemented in the QUANTUM-ESPRESSO code.<sup>13,14</sup> All elements are represented by norm-conserving, optimized nonlocal pseudopotentials with a cutoff energy of 50 Ry, generated with the OPIUM package.<sup>15</sup> The polarization was calculated following the Berry-phase approach<sup>16,17</sup> by choosing an adiabatic path from the centrosymmetric reference state to the equilibrium polarized state.  $8 \times 8 \times 8$  Monkhorst-Pack *k*-point grids were used to sample the Brillouin zone, while the polarization was calculated with  $6 \times 6 \times 20$  *k*-point grids, where the denser grids are for the polarization direction.<sup>18</sup> We also used two hybrid functionals: HSE06 and PBE0, to corroborate the band gap change trend that we find.<sup>11,19-21</sup> Note that the band gap here was estimated using the single-particle Kohn-Sham eigenvalues, which, although theoretically not fully justified, can be compared to the fundamental band gap obtained by photoemission or electrochemical measurements.<sup>22</sup> We adopted a five-atom unit cell for both the *R* and *T* phase perovskites and fully relaxed the structures. For some perovskites (e.g., BaTiO<sub>3</sub>), the experimentally found *T* phase is due to the averaging of local *R* cation displacements.<sup>23</sup> For these cases, the *T* phase studied in our five-atom calculations should be thought of as a local *T* phase that does not correspond to the experimental *T* phase but can be achieved in epitaxially strained thin films. For other perovskites (e.g., BaZrO<sub>3</sub>), the ground state structure involves octahedral rotations that cannot be represented in a five-atom unit cell. Nevertheless, we used the simple five-atom cells on purpose to isolate the effects of *B*-cation displacements from the effects of other ABO<sub>3</sub> distortions.

Table I shows the calculated band gaps and polarizations of the *T* and *R* phases of various ABO<sub>3</sub> perovskites using three different methods. The electronic structure of typical

<sup>a)</sup>fenggong@sas.upenn.edu

<sup>b)</sup>rappe@sas.upenn.edu

TABLE I. The band gaps  $E_g$  (eV) of various rhombohedral ( $R$ ) and tetragonal ( $T$ ) oxides calculated with various functionals. The polarization ( $C/m^2$ ) calculated at the GGA level is also shown.  $\text{LaScO}_3$ ,  $\text{BaTiO}_3$ ,  $\text{PbTiO}_3$ ,  $\text{KNbO}_3$ , and  $\text{WO}_3$  are from fully relaxed structures while  $\text{BaZrO}_3$  and  $\text{KTaO}_3$  are relaxed starting from the  $\text{BaTiO}_3$  and  $\text{KNbO}_3$  structures.

Composition	$E_g^{\text{GGA}}$		$E_g^{\text{HSE06}}$		$E_g^{\text{PBE0}}$		$P^{\text{GGA}}$	
	$R$	$T$	$R$	$T$	$R$	$T$	$R$	$T$
$\text{LaScO}_3$	3.49	3.36	5.16	5.08	5.89	5.82	0.29	0.20
$\text{BaTiO}_3$	2.30	1.74	3.72	3.12	4.46	3.86	0.40	0.28
$\text{BaZrO}_3$	3.56	3.04	5.04	4.51	5.77	5.24	0.32	0.22
$\text{PbTiO}_3$	2.29	1.70	3.51	2.92	4.19	3.63	0.72	0.97
$\text{KTaO}_3$	3.29	2.32	4.73	3.72	5.47	4.45	0.51	0.46
$\text{KNbO}_3$	2.40	1.39	3.68	2.60	4.42	3.32	0.56	0.50
$\text{WO}_3$	1.92	0.76	3.13	1.86	3.87	2.59	0.64	0.54

$\text{ABO}_3$  perovskites depends on the fundamental characteristics of the metal-oxygen chemical bonds. Because of the large electronegativity difference between oxygen and the metals, the band gap of a perovskite can be as large as  $>5$  eV (e.g., 5.72 eV for  $\text{LaScO}_3$ ). Basically, the top of the valence band (VB) arises mainly from the O  $2p$  orbitals, while the bottom of the conduction band (CB) is essentially set by the  $B$ -cation  $d$  orbitals. Compared to the  $A$ -cation, the  $B$ -cation has a much more significant effect on fixing the band gaps. For example, the GGA band gap of rhombohedral  $\text{BaZrO}_3$  is 1.3 eV larger than that of  $\text{BaTiO}_3$  because Zr is less electronegative than Ti. Similarly, the band gap of  $\text{KTaO}_3$  is around 0.9 eV larger than that of  $\text{KNbO}_3$ . Nevertheless,  $\text{BaTiO}_3$  and  $\text{PbTiO}_3$  have similar band gaps even though the electronegativity of Pb is much higher than that of Ba, suggesting a minor role of  $A$ -O chemical bonds in determining the band gaps.

Additionally, the band gaps of different phases of perovskites with the same composition can be quite different, indicating a more complex picture of the crystal structure and electronic structure in perovskites. Specifically, we find that the  $R$  perovskite phase always exhibits a larger band gap than its  $T$  counterpart irrespective of the composition (Fig. 1). The band gap difference between the  $R$  and  $T$  perovskites ranges from 0.1 eV for  $\text{LaScO}_3$  to 1.2 eV for  $\text{WO}_3$  using GGA (Table II). This trend is very robust and further corroborated by the hybrid functional calculations using HSE06 and PBE0. The HSE06 band gaps are 1.1–1.5 eV larger than the GGA gaps, while PBE0 increases the band gaps further by about 0.7 eV. However, the band gap differences change by less than 0.15 eV as the functional is varied. Fig. 1(b)

TABLE II. The band gap difference  $E_g^R - E_g^T$  between  $R$  and  $T$  perovskite oxides with various functionals.

	$\text{LaScO}_3$	$\text{BaTiO}_3$	$\text{BaZrO}_3$	$\text{PbTiO}_3$	$\text{KTaO}_3$	$\text{KNbO}_3$	$\text{WO}_3$
GGA	0.13	0.56	0.59	0.68	0.97	1.01	1.18
HSE06	0.08	0.60	0.59	0.68	1.01	1.08	1.29
PBE0	0.07	0.60	0.56	0.65	1.02	1.10	1.30

shows the band gap difference as a function of the  $B$ -cation valence. As the  $B$ -cation valence increases from  $+3$  to  $+6$ , the band gap difference is also substantially enlarged. Furthermore, the polarizations of the  $R$  perovskites are also uniformly enhanced except for  $\text{PbTiO}_3$  (Fig. 1). Thus, the band gaps of perovskite oxides can be reduced by a large amount while the polarizations are still largely retained as they undergo the local  $R$ -to- $T$  phase transitions.

To further investigate the origin of the large band gap difference between  $R$  and  $T$  perovskites, we plot the band structure and density of states (DOS) of  $\text{BaTiO}_3$  (Fig. 2). Clearly, the band gap reduction from  $R$  to  $T$  phase arises from the down-shift of the CB since the VB is essentially unchanged. As shown in Fig. 2(a), the bottom of the CB in a perovskite oxide falls at the  $\Gamma$  point due to the essentially nonbonding  $B$ -O interaction constrained by the translational symmetry. At the  $A$  point, the  $B$ -O interaction is mainly antibonding. The contrast of the orbital character between the  $\Gamma$  and  $A$  points determines the CB width and the resulting band gap. As the  $B$ -cations move further off-center in the  $R$  phase, long vs. short bond length differences become significant along all the three crystallographic directions. Simultaneously, both  $O$ - $B$ - $O$  and  $B$ - $O$ - $B$  angles deviate severely from  $180^\circ$  and more antibonding character is induced at  $\Gamma$ -point by the distortion of the  $O$ - $B$  orbital overlap.<sup>9</sup> Therefore, the bottom of the CB shifts up due to the enhanced antibonding interaction. This enhancement of the antibonding  $O$ - $B$  interaction is increased as the valence of the  $B$ -cation increases. This is because when the  $B$ -cation changes from  $\text{Sc}^{3+}$  to  $\text{W}^{6+}$ , the electronegativity of the  $B$ -metal rises, leading to more covalent  $B$ - $O$  bonds. Overall, the band gaps are substantially increased as the CB involves more antibonding character in the  $R$  phase.

To elucidate the connections between structural distortions and polarization, we carefully analyze the  $\text{BO}_6$  distortions in perovskites. Basically, there are two kinds of  $\text{BO}_6$  octahedral distortions: octahedral tilting and  $B$ -cation off-center displacement. In some materials (such as monoclinic  $\text{WO}_3$ ), both  $\text{BO}_6$  octahedral tilting and  $B$ -cation

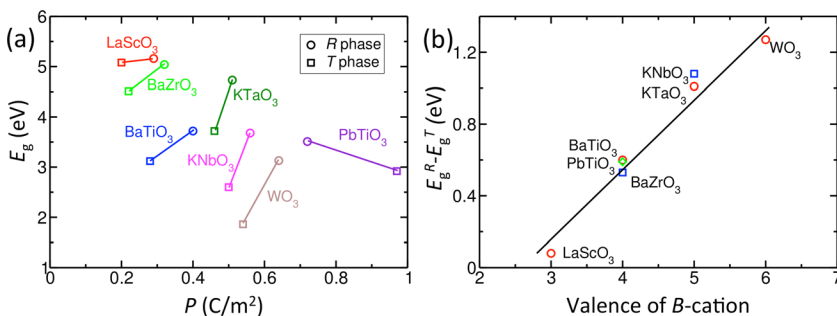


FIG. 1. (a) The HSE06 band gap (eV) as a function of the polarization ( $C/m^2$ ) in  $T$  and  $R$  perovskite oxides and (b) the band gap difference  $E_g^R - E_g^T$  as a function of the valence of the  $B$ -cation.

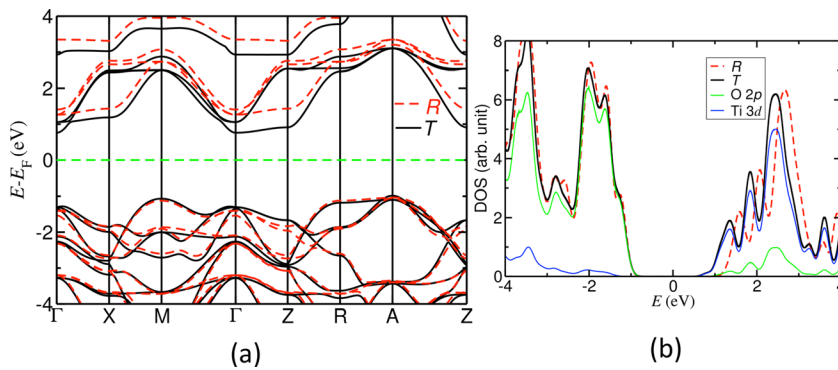


FIG. 2. The band structure and DOS of tetragonal (*T*) and rhombohedral (*R*) BaTiO<sub>3</sub>.

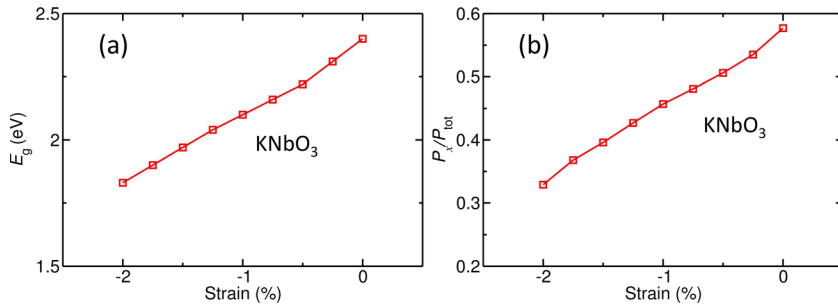


FIG. 3. The (a) band gap  $E_g$  (eV) and (b) ratio between the  $x$ -component of  $P$  and the total  $P$  ( $P_x/P_{tot}$ ) as a function of the in-plane strain.

off-center displacements can exist.<sup>22</sup> Octahedral tiltings with deviation of the  $B$ - $O$ - $B$  angles from  $180^\circ$  can substantially affect the electronic structure of perovskites, even though they induce no polarization in simple  $ABO_3$ . On the other hand,  $B$ -cation off-center displacements could lead to long and short bond length differences, deviations of both  $O$ - $B$ - $O$  and  $B$ - $O$ - $B$  angles from  $180^\circ$ , and significant polarization. In *T* phase perovskites, the  $B$ -cations are displaced along the  $[001]$  direction while in the *R* phase the off-centering is along all the three Cartesian directions. Correspondingly, in the *T* phase both the  $O$ - $B$ - $O$  and  $B$ - $O$ - $B$  angles are still  $180^\circ$  along the  $[001]$  direction while in the *R* phase they deviate from  $180^\circ$  along all the three crystallographic directions. This leads to smaller band gaps in the *T* phase.

The local *T* phase displacements necessary for lower  $E_g$  could be achieved by strain, doping,<sup>24</sup> or by mixing with locally tetragonal materials such as PbTiO<sub>3</sub> in a solid solution. Here, we examine the effect of strain. As shown in Fig. 3, as the in-plane compressive strain increases, the band gap of KNbO<sub>3</sub> decreases, and the proportion of the in-plane component to the total polarization also decreases. This verifies the feasibility of our proposed band gap engineering strategy using the *R*-to-*T* phase transition.

In summary, we propose a way to engineer the band gap of perovskites from first principles. Through *R*-to-*T* phase transitions, the band gaps can be significantly reduced by up to 1.2 eV without significantly affecting the magnitude of polarizations. The  $BO_6$  distortions, especially the  $B$ -cation off-center displacements, enhance the antibonding character of the CB, leading to wider band gaps in the *R* phase. The clear correlation between the structure, electronic structure, and polarization provides a route for the design of photovoltaic perovskite FEs.

F.W. was supported by the National Science Foundation, under Grant No. DMR11-24696. I.G. was supported by the

Office of Naval Research, under Grant No. N00014-12-1-1033. A.M.R. was supported by the Office of Naval Research under Grant No. N00014-11-1-0664. Computational support was provided by the National Energy Research Scientific Computing Center of the Department of Energy and the High-Performance Computing Modernization Office of the Department of Defense.

- <sup>1</sup>K. Maeda, K. Teramura, D. Lu, T. Takata, N. Saito, Y. Inoue, and K. Domen, *Nature* **440**, 295 (2006).
- <sup>2</sup>V. M. Fridkin, *Crystallogr. Rep.* **46**, 654 (2001).
- <sup>3</sup>A. M. Glass, D. von der Linde, and T. J. Negran, *Appl. Phys. Lett.* **25**, 233 (1974).
- <sup>4</sup>A. G. Chynoweth, *Phys. Rev.* **102**, 705 (1956).
- <sup>5</sup>I. Grinberg, D. V. West, M. Torres, G. Gou, D. M. Stein, L. Wu, G. Chen, E. M. Gallo, A. R. Akbashev, P. K. Davies, J. E. Spanier, and A. M. Rappe, *Nature* **503**, 509 (2013).
- <sup>6</sup>W. S. Choi, M. F. Chisholm, D. J. Singh, T. Choi, and G. E. Jellison, *Nat. Commun.* **3**, 689 (2012).
- <sup>7</sup>M. A. Pena and J. L. G. Fierro, *Chem. Rev.* **101**, 1981 (2001).
- <sup>8</sup>A. Ohtomo and H. Y. Hwang, *Nature* **427**, 423 (2004).
- <sup>9</sup>H. W. Eng, P. W. Barnes, B. M. Auer, and P. M. Woodward, *J. Solid State Chem.* **175**, 94 (2003).
- <sup>10</sup>A. Y. Borisevich, H. J. Chang, M. Huijben, M. P. Oxley, S. Okamoto, M. K. Niranjan, J. D. Burton, E. Y. Tsymlal, Y. H. Chu, P. Yu, R. Ramesh, S. V. Kalinin, and S. J. Pennycook, *Phys. Rev. Lett.* **105**, 087204 (2010).
- <sup>11</sup>J. P. Perdew, K. Burke, and M. Ernzerhof, *Phys. Rev. Lett.* **77**, 3865 (1996).
- <sup>12</sup>J. P. Perdew, K. Burke, and M. Ernzerhof, *Phys. Rev. Lett.* **78**, 1396 (1997).
- <sup>13</sup>P. Giannozzi, S. Baroni, N. Bonini, M. Calandra, R. Car, C. Cavazzoni, D. Ceresoli, G. L. Chiarotti, M. Cococcioni, I. Dabo, A. D. Corso, S. de Gironcoli, S. Fabris, G. Fratesi, R. Gebauer, U. Gerstmann, C. Gougousis, A. Kokalj, M. Lazzeri, L. Martin-Samos, N. Marzari, F. Mauri, R. Mazzarello, S. Paolini, A. Pasquarello, L. Paulatto, C. Sbraccia, S. Scandolo, G. Sclauzero, A. P. Seitsonen, A. Smogunov, P. Umari, and R. M. Wentzcovitch, *J. Phys.: Condens. Matter* **21**, 395502 (2009).
- <sup>14</sup>W. Kohn and L. J. Sham, *Phys. Rev.* **140**, A1133 (1965).
- <sup>15</sup>A. M. Rappe, K. M. Rabe, E. Kaxiras, and J. D. Joannopoulos, *Phys. Rev. B* **41**, 1227 (1990).
- <sup>16</sup>R. D. King-Smith and D. Vanderbilt, *Phys. Rev. B* **47**, 1651 (1993).
- <sup>17</sup>R. Resta, *Ferroelectrics* **136**, 51 (1992).

<sup>18</sup>H. J. Monkhorst and J. D. Pack, *Phys. Rev. B* **13**, 5188 (1976).

<sup>19</sup>K. A. Johnson and N. W. Ashcroft, *Phys. Rev. B* **58**, 15548 (1998).

<sup>20</sup>J. Heyd, G. E. Scuseria, and M. Ernzerhof, *J. Chem. Phys.* **118**, 8207 (2003).

<sup>21</sup>J. Heyd, G. E. Scuseria, and M. Ernzerhof, *J. Chem. Phys.* **124**, 219906 (2006).

<sup>22</sup>F. Wang, C. Di Valentin, and G. Pacchioni, *J. Phys. Chem. C* **115**, 8345 (2011).

<sup>23</sup>T. Egami, W. Dmowski, M. Akbas, and P. K. Davies, in *First-Principles Calculations for Ferroelectrics-Fifth Williamsburg Workshop*, edited by R. E. Cohen (American Institute for Physics, Melville, New York, 1998), pp. 1–10.

<sup>24</sup>S. Tosoni, C. Di Valentin, and G. Pacchioni, *J. Phys. Chem. C* **118**, 3000 (2014).